Enhanced Ionization of Embedded Clusters by Electron-Transfer-Mediated Decay in Helium Nanodroplets

A. C. LaForge,[1,*] V. Stumpf,[2] K. Gokhberg,[2] J. von Vangerow,[1] F. Stienkemeier,[1] N. V. Kryzhevoi,[2] P. O'Keeffe,[3] A. Ciavardini,[3] S. R. Krishnan,[4] M. Coreno,[3] K. C. Prince,[5] R. Richter,[5] R. Moshammer,[6] T. Pfeifer,[6] L. S. Cederbaum,[2] and M. Mudrich[1]

[1]*Physikalisches Institut, Universität Freiburg, 79104 Freiburg, Germany*
[2]*Physikalisch-Chemisches Institut, Universität Heidelberg, 69120 Heidelberg, Germany*
[3]*CNR—Istituto di Struttura della Materia, CP10, 00016 Monterotondo Scalo, Italy*
[4]*Department of Physics, Indian Institute of Technology, Madras, Chennai 600 036, India*
[5]*Elettra-Sincrotrone Trieste, Basovizza, Trieste 34149, Italy*
[6]*Max-Planck-Institut für Kernphysik, 69117 Heidelberg, Germany*

(Received 15 December 2015; published 19 May 2016)

We report the observation of electron-transfer-mediated decay (ETMD) involving magnesium (Mg) clusters embedded in helium (He) nanodroplets. ETMD is initiated by the ionization of He followed by removal of two electrons from the Mg clusters of which one is transferred to the He ion while the other electron is emitted into the continuum. The process is shown to be the dominant ionization mechanism for embedded clusters for photon energies above the ionization potential of He. For Mg clusters larger than five atoms we observe stable doubly ionized clusters. Thus, ETMD provides an efficient pathway to the formation of doubly ionized cold species in doped nanodroplets.

DOI: 10.1103/PhysRevLett.116.203001

The interplay between electrons after single photon absorption has been a stimulating topic in atomic physics since its foundation. Specifically, processes such as shake-off in single photon double ionization [1], postcollision interaction in Auger processes [2], and autoionization of doubly excited states [3] have been a fertile ground for studying electron correlation. Systems consisting of many weakly interacting atoms or molecules additionally offer a unique environment for studying this correlation where new decay mechanisms, unavailable in atomic systems, become accessible between the constituents. In particular, Cederbaum and co-workers [4] theoretically predicted a new decay mechanism, known as interatomic Coulombic decay (ICD), available in electronically excited weakly bound systems. In the case where local electronic decay is energetically forbidden, ICD offers a new ultrafast decay path typically on the femtosecond time scale where energy is exchanged with a neighboring atom leading to its ionization. Since its proposition [4] and experimental confirmation [5,6], ICD has been observed in a wide variety of weakly bound systems including, for example, helium (He) dimers [7,8] and water clusters [9,10]. For reviews, see [11,12].

Electron-transfer-mediated decay (ETMD), theoretically predicted [13] and recently experimentally observed [14,15], is another interatomic decay mechanism accessible upon ionization in weakly bound systems. Electron transfer from the neighbor to the ion releases energy that is utilized to either (i) directly emit a second electron [ETMD(2)] or (ii) emit an electron from a second neighbor, ETMD(3). Importantly, ETMD is a much stronger decay channel than its radiative counterpart. The original version of ETMD applies to ions in an excited state that possess sufficient excess energy to ionize their neighbors. In this case, ETMD is quenched by ICD due to a large difference in the respective rates [16]. Recently, a new variant of ETMD was reported that does not require the aforementioned excess energy and can even occur for a ground state ion [17]. This is distinct from simple charge transfer as it is a two electron process, and since for such states ICD is impossible, ETMD was shown to be the leading decay process.

Recently, Stumpf *et al.* [18] predicted ETMD dramatically enhances (by ~3 orders of magnitude) the single photon double ionization of a magnesium (Mg) atom in the vicinity of a He atom. In this case, ETMD proceeds by the initial ionization of a He atom followed by ETMD of the neighboring Mg atom yielding Mg^{2+} and neutral He. Surprisingly, due to ETMD, the theoretical cross section for double ionization of Mg is even higher than that of direct single ionization and is comparable to that of He. Overall, the decay path and its predicted enhancement is not limited to Mg in He clusters, but can be applied to any embedded atoms or molecules that have a lower double ionization potential than the single ionization potential of the environment. Thus, the phenomenon is considered to be of quite general relevance and can be used in He droplets as a new pathway to the formation of doubly ionized cold species that are difficult to form otherwise.

Here, we report on the first experimental observation of ETMD of particles embedded in superfluid He nanodroplets. Following the initial ionization of a He atom within the droplet, ETMD leads to double ionization of the embedded Mg clusters. The electron kinetic energy spectra reveal a low-energy ETMD peak at about 1 eV agreeing well with theory. The ETMD mechanism turns out to be a dominant means to doubly ionize Mg clusters within the droplets, allowing the investigation of the stability of doubly ionized Mg clusters.

He droplets have been used wisely as cold, weakly perturbing matrices for studies in spectroscopy and chemical dynamics of embedded atoms and molecules [19,20]. While typically the He environment is inert to the embedded species, when the droplet is excited or ionized the situation is completely different and the droplet becomes a highly reactive medium to the embedded species [21]. Even doubly ionized dopants have recently been observed due to sequential collisions of metastable He atoms produced in a single droplet by electron bombardment [22].

The experiment was performed using a mobile He droplet machine attached to an imaging photoelectron-photoion coincidence (PEPICO) detector at the GasPhase beamline of Elettra-Sincrotrone Trieste, Italy. The setup has been described in some detail [23,24], and only the significant points are addressed here. In short, a beam of He nanodroplets is produced by continuously expanding pressurized (50 bar), high purity He out of a cryogenic nozzle with 5 μm diameter. Under these expansion conditions, the mean droplet sizes range from 10^1 to 10^{11} He atoms per droplet [19]. After passing a skimmer (0.4 mm) and a mechanical beam chopper used for discriminating the droplet beam signal from the He background, the droplets were doped using the "pickup" technique [25] with an oven cell filled with Mg heated to generate partial pressures where one to 25 Mg atoms were attached to the droplets. While most atomic and molecular species become submerged in the interior of He nanodroplets, alkaline earth atoms such as Mg remain weakly bound inside the surface layer [26]. The He droplet beam next crosses the synchrotron beam at the focus of the PEPICO detector consisting of an ion time-of-flight detector and velocity map imaging detector operating in coincidence. With such a detection technique, one can record electron kinetic energy distributions in coincidence with specific ion masses in multi-coincidence mode [23]. The kinetic energy distributions were reconstructed using a standard Abel inversion method [27]. The photon energy was tuned by scanning the monochromator and gap of the undulator simultaneously with a typical step size of 20 meV and energy resolution $E/\Delta E \approx 10^4$. The radiation intensity was monitored by a calibrated photodiode and all photon energy dependent ion and electron spectra shown in this work are normalized to this intensity signal. Additionally, the photon flux was sufficiently low to ensure that no more than one photon per droplet was absorbed.

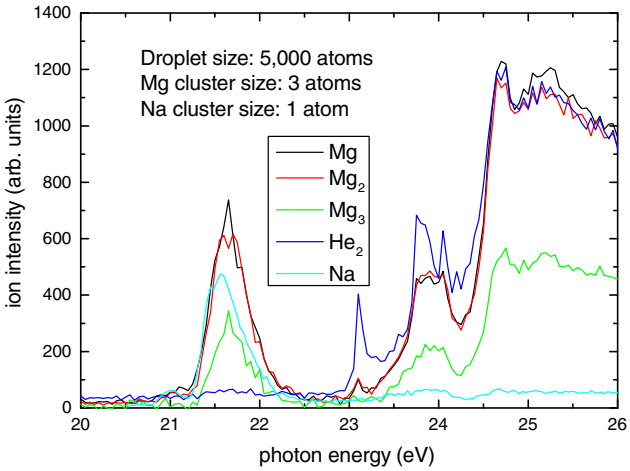

FIG. 1. Ion signal intensity of Mg^+ (black), Mg_2^+ (red), Mg_3^+ (green), Na^+ (cyan), and He_2^+ (blue) as a function of photon energy. The droplet size is 5000 He atoms with either an average of two to three Mg atoms or one Na atom attached.

Figure 1 shows the ion signal intensities of Mg^+, Mg_2^+, Mg_3^+, and He_2^+ as a function of photon energy. The droplet size is 5000 He atoms with an average of two to three Mg atoms attached. The photon energy was tuned from 20 to 26 eV, which covers energies below the lowest dipole-allowed excitation energy (21.2 eV) to above the atomic ionization threshold (24.6 eV) of He [28]. The observed He_2 ion signals are similar to previous synchrotron results [29,30], where for energies below about 23 eV (the adiabatic ionization potential of He droplets) the signal is nearly 0. At energies higher than 23 eV but below the ionization threshold of atomic He ($h\nu \leq 24.6$ eV), ionization occurs through He dimerization followed by autoionization [30].

There are several mechanisms leading to single ionization of Mg atoms and clusters embedded in He droplets. First, direct single ionization above 7.6 eV and double ionization above 22.7 eV are possible [31]. Additionally, the He environment opens new pathways to ionization. When the droplet is resonantly excited [28], ionization proceeds through Penning or ICD [32,33] processes. When the droplet is ionized, electron transfer can ionize the dopant. For high enough photon energies, electron impact ionization of the dopant is possible by photoelectrons produced in the initial ionization of the He droplet. All the processes above lead to the production of a single Mg^+ or Mg_n^+ ion by a single photon. A single photon can also doubly ionize Mg_n via ETMD [18]. The thus produced Mg_n^{2+} can either fragment into two singly charged fragments or remain a stable dication.

For the Mg^+ ions below 21 eV photon energy, no signal was observed; therefore, direct ionization of Mg is negligible. Around 21.6 eV, there is a large peak in all three Mg

ion signals in Fig. 1 corresponding to ionization by Penning or ICD processes [32,33] as the He atoms are excited to the droplet equivalent of the $1s2p$ state [28]. At higher photon energies, the Mg ion signals closely follow the He_2^+ ion signal pointing to He-mediated ionization of Mg. Previous experiments with dopants (alkali metals) that cannot undergo ETMD exhibit efficient dopant ionization at the excitation energies of the droplet. However, ionization of the dopant was comparatively weak at higher photon energies above the droplet's ionization threshold in contrast to the case of Mg presented here [24,34]. For comparison, the ion intensity of a single sodium (Na) atom, the alkali analog to Mg, attached to the same sized He droplet is shown in Fig. 1. Although similar intensities are observed around 21.6 eV by energy transfer, the intensities above the droplet ionzation threshold are well over an order of magnitude smaller. This is surprising considering that the cross section for resonant excitation of He [29] is three times higher than the ionization cross section near threshold [35] and that Mg is located close to the droplet's surface similar to alkali metals [36]. The question that arises is whether the strong enhancement is due to ETMD.

To address the differences in the ionization mechanisms discussed above, we show in Fig. 2(a) the mass spectra for photon energies of 40 (black line) and 21.5 eV (red line) for droplets consisting of 50 000 He atoms with an average of five to six Mg atoms attached. For both energies, a large contribution of Mg ions is observed in the mass spectra, and, similar to Fig. 1, there are substantially higher signals above the ionization threshold ($h\nu = 40$ eV). Here, Mg^+-He complexes are observed at multiples of 4 amu in the mass spectra following multiples of the Mg mass (24 amu).

Importantly, at higher masses, broad peaks at half-integer values of the mass-to-charge ratio appear. These are due to the formation of doubly ionized Mg clusters with at least five atoms. The stability of doubly ionized clusters has previously been studied [37,38] and it was experimentally shown that Mg clusters consisting of five atoms or more are sufficiently long lived to be detected in a mass spectrometer. The signals in the mass spectrum corresponding to integer numbers of Mg atoms in Mg_n^+ may, of course, also be due to Mg_{2n}^{2+}. However, it is impossible to disentangle them from singly ionized clusters. The observation of doubly ionized Mg clusters gives the first direct evidence of ETMD for this system.

In order to identify the various ionization mechanisms, mass-correlated electron spectra are shown in Fig. 2(b) for Mg_n^{2+} (black line). As there was no difference between the electron spectra correlated to the various doubly ionized clusters, they were combined to increase statistics. At 15.4 eV, one observes a large photoelectron peak resulting from the initial ionization of He [$h\nu - E_i(\mathrm{He}) = 15.4$ eV]. The Mg_n^{2+} peak at low energy is due to ETMD as the electrons emitted in this process lie in the observed energy

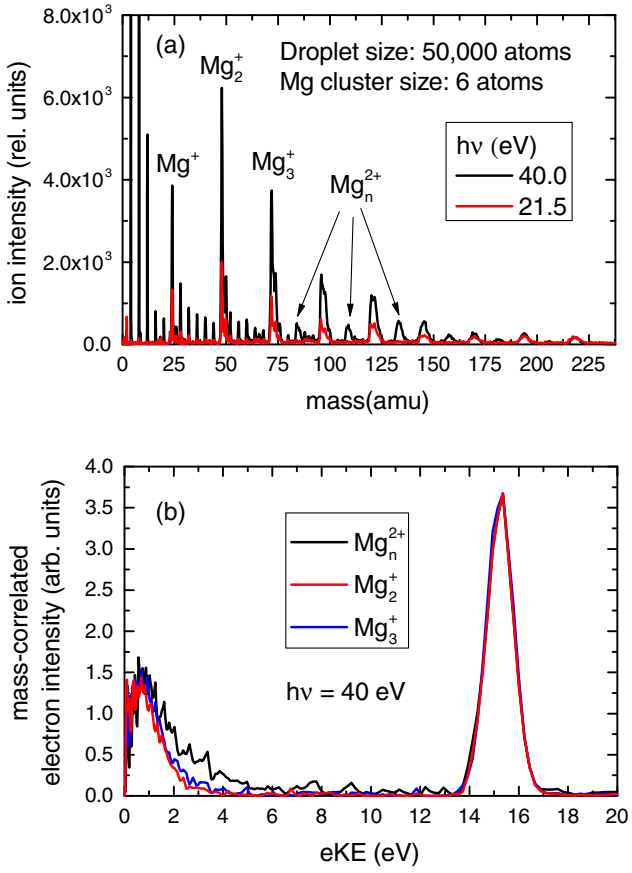

FIG. 2. (a) Mass spectra of He droplets doped with Mg clusters at photon energies of 40 (black) and 21.5 eV (red). The droplet size is 50 000 He atoms with an average of five to six Mg atoms attached. (b) Electron kinetic energy distributions measured in coincidence with single ions for $Mg_{n=7,9,11}^{2+}$ (black line), Mg_2^+ (red line), and Mg_3^+ (blue line).

range (see Supplemental Material and Ref. [18]) and there are no other mechanisms that produce an electron peak in this energy range. We argue below that ETMD is by far the dominant mechanism for producing doubly ionized Mg clusters. Shown in Fig. 2(b) are also the mass-correlated electron spectra for the Mg_2^+ (red line) and Mg_3^+ (blue line) ions. Surprisingly, they are similar to that of Mg_n^{2+}, exhibiting a photoelectron peak at 15.4 eV and a low-energy peak at about 1 eV. Therefore, not only is ETMD responsible for the doubly ionized clusters in the mass spectra but it could be a primary mechanism for the production of singly charged smaller clusters, which result upon fragmentation of doubly ionized unstable clusters. There is a slight discrepancy between the spectra for Mg_n^{2+} and those of smaller clusters, Mg_2^+ and Mg_3^+; namely, the ETMD peak for Mg_n^{2+} extends to higher energies. The additional energy for Mg_n^{2+} clusters is due to the clusters not undergoing dissociation, which requires additional energy. The Supplemental Material contains mass and electron spectra similar to those shown in Fig. 2 for

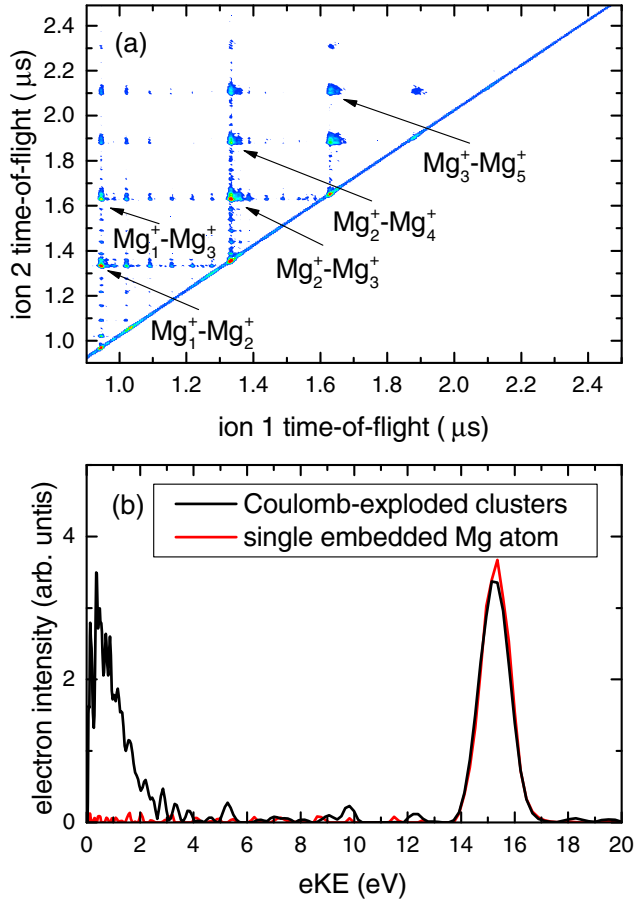

FIG. 3. (a) Ion-ion coincidence time-of-flight spectrum and (b) electron spectrum correlated to Mg_m^+-Mg_n^+ ion-ion coincidences (black line). The photon energy is 40 eV. The droplet size is 50 000 He atoms with an average of six Mg atoms attached. Electron spectra are correlated to a single Mg atom (red line) embedded in a droplet of size 5000 atoms.

5000 He atoms, but with an average of two to three Mg atoms attached. In this case, Mg_5^{2+} can clearly be identified in the mass spectra.

Figure 3(a) shows the ion-ion coincidence time-of-flight spectrum for He droplets consisting of 50 000 atoms doped with an average of five to six Mg atoms. The photon energy was 40 eV. As the flight times of the respective ions are symmetric, the coincidence map is folded along the axis of symmetry. The peak shapes observed in the spectra give information about the dissociation process [39]. Additionally, due to the dense He environment, the kinetic energy of Coulomb-exploded molecules embedded in He droplets is significantly damped. The coincidence map is centered around Coulomb-exploded Mg oligomers. Because of the dead time of the detector (≈9 ns), there is a significant loss of statistics for ions of equal mass lying along the axis of symmetry. Therefore, the focus of our results is on Coulomb-exploded clusters of unequal masses, $Mg_m^+ - Mg_n^+$, where $n \neq m$. Overall, the coincidence map reveals a rich spectrum of doubly ionized clusters up to Mg_9 showing that many of the singly ionized Mg ions seen in Fig. 2(a) stem from larger doubly ionized clusters.

Figure 3(b) shows the electron spectra correlated to ion-ion coincidences (black line). Since there was no substantial change (e.g., peak position and width or relative ratio of the ETMD to photoelectron peak) for the various Mg ion-ion pairs, the individual electron spectra were summed for all large heterogeneous ion-ion pairs shown in the coincidence map in Fig. 3(a). Similar to the electron spectra shown in Fig. 2(b), the ETMD peak is also centered at 0.9 eV. Here, the ratio of the integrated ETMD peak to the photoelectron peak is 81% in this case, significantly higher than that shown in Fig. 2(b) (35%–50% depending on the correlated ion), consistent with the fact that doubly ionized clusters are a result of ETMD. The most likely reason that the ratio of the ETMD to photoelectron peak is less than unity is the large amount of false coincidences from ionized He. Besides the photoelectron and ETMD peaks, there are no electron signals from other mechanisms, which highlights that ETMD is the dominant process for double ionization of Mg clusters. The ion-ion coincidence map and electron spectra for He droplets consisting of 5000 atoms doped with on average two to three Mg atoms are given in Supplemental Material and give consistent results with those in Fig. 3.

So far, we have solely focused on Mg clusters embedded in He nanodroplets where we have shown that the He environment dramatically enhances the double ionization of the cluster due to ETMD. Finally, we address the enhancement of the double ionization efficiency of a single Mg atom with a single He atom as a neighbor very recently investigated by Stumpf *et al.* [18]. We observed no doubly ionized Mg atoms when only a single Mg atom is embedded in the nanodroplet; see Supplemental Material. The Mg^+-correlated electron spectra for a single Mg atom embedded in a droplet consisting of 5000 atoms are shown in Fig. 3(b). In this case, the ETMD electron peak was absent, suggesting that ionization proceeds exclusively through electron transfer. Thus, ETMD appears to be inactive for single Mg atoms attached to He droplets.

We attribute this to the ultrafast formation of He_2^+ in the droplet, which is predicted to occur in 60–80 fs after the initial ionization [24]. Our calculations show clearly that the ETMD channel for a single Mg atom is closed once He_2^+ is formed. Additionally included in the Supplemental Material are theoretical calculations of the ETMD electron kinetic energy for the most likely configurations between He_2^+ and a Mg trimer where ETMD can still occur. It is still inconclusive whether ETMD can occur for Mg dimers.

In conclusion, electron-transfer-mediated decay was observed for Mg clusters embedded in He droplets. This decay channel was shown to be a dominant ionization mechanism for energies above the ionization threshold of He. For clusters of five Mg atoms and greater, stable, doubly ionized Mg clusters were observed after ETMD.

For single Mg atoms embedded in nanodroplets, the ETMD channel is closed due to the ultrafast formation of an equilibrated He dimer ion. In general, ETMD offers a novel method for producing doubly ionized systems if the environment has a higher single ionization threshold.

The authors gratefully acknowledge the staff of Elettra-Sincrotrone Trieste for providing high-quality light. A. C. L., J. V. V., and M. M. gratefully acknowledge the financial support of Deutsche Forschungsgemeinschaft (DFG) (Grant No. MU 2347/10-1). V. S. and K. G. gratefully acknowledge the financial support of DFG (research unit 1789). L. S. C. gratefully acknowledges the funding from the European Research Council (ERC) Advanced Investigator Grant No. 692657 [40–47].

*aaron.laforge@physik.uni-freiburg.de

[1] T. Pattard, T. Schneider, and J. Rost, J. Phys. B **36**, L189 (2003).
[2] A. Russek and W. Mehlhorn, J. Phys. B **19**, 911 (1986).
[3] R. Madden and K. Codling, Phys. Rev. Lett. **10**, 516 (1963).
[4] L. S. Cederbaum, J. Zobeley, and F. Tarantelli, Phys. Rev. Lett. **79**, 4778 (1997).
[5] S. Marburger, O. Kugeler, U. Hergenhahn, and T. Möller, Phys. Rev. Lett. **90**, 203401 (2003).
[6] T. Jahnke *et al.*, Phys. Rev. Lett. **93**, 163401 (2004).
[7] N. Sisourat, N. V. Kryzhevoi, P. Kolorenč, S. Scheit, T. Jahnke, and L. S. Cederbaum, Nat. Phys. **6**, 508 (2010).
[8] T. Havermeier *et al.*, Phys. Rev. Lett. **104**, 133401 (2010).
[9] T. Jahnke *et al.*, Nat. Phys. **6**, 139 (2010).
[10] M. Mucke, M. Braune, S. Barth, M. Förstel, T. Lischke, V. Ulrich, T. Arion, U. Becker, A. Bradshaw, and U. Hergenhahn, Nat. Phys. **6**, 143 (2010).
[11] U. Hergenhahn, J. Electron Spectrosc. Relat. Phenom. **184**, 78 (2011).
[12] T. Jahnke, J. Phys. B **48**, 082001 (2015).
[13] J. Zobeley, R. Santra, and L. S. Cederbaum, J. Chem. Phys. **115**, 5076 (2001).
[14] K. Sakai *et al.*, Phys. Rev. Lett. **106**, 033401 (2011).
[15] M. Förstel, M. Mucke, T. Arion, A. M. Bradshaw, and U. Hergenhahn, Phys. Rev. Lett. **106**, 033402 (2011).
[16] V. Averbukh and L. S. Cederbaum, J. Chem. Phys. **123**, 204107 (2005).
[17] V. Stumpf, P. Kolorenč, K. Gokhberg, and L. S. Cederbaum, Phys. Rev. Lett. **110**, 258302 (2013).
[18] V. Stumpf, N. V. Kryzhevoi, K. Gokhberg, and L. S. Cederbaum, Phys. Rev. Lett. **112**, 193001 (2014).
[19] J. P. Toennies and A. F. Vilesov, Angew. Chem., Int. Ed. Engl. **43**, 2622 (2004).
[20] F. Stienkemeier and K. K. Lehmann, J. Phys. B **39**, R127 (2006).
[21] M. Mudrich and F. Stienkemeier, Int. Rev. Phys. Chem. **33**, 301 (2014).
[22] H. Schöbel *et al.*, Phys. Rev. Lett. **105**, 243402 (2010).
[23] P. O'Keeffe *et al.*, Rev. Sci. Instrum. **82**, 033109 (2011).
[24] D. Buchta *et al.*, J. Phys. Chem. **117**, 4394 (2013).
[25] T. Gough, M. Mengel, P. Rowntree, and G. Scoles, J. Chem. Phys. **83**, 4958 (1985).
[26] M. Barranco, R. Guardiola, S. Hernández, R. Mayol, J. Navarro, and M. Pi, J. Low Temp. Phys. **142**, 1 (2006).
[27] G. A. Garcia, L. Nahon, and I. Powis, Rev. Sci. Instrum. **75**, 4989 (2004).
[28] M. Joppien, R. Karnbach, and T. Möller, Phys. Rev. Lett. **71**, 2654 (1993).
[29] D. Buchta *et al.*, J. Chem. Phys. **139**, 084301 (2013).
[30] R. Fröchtenicht, U. Henne, J. P. Toennies, A. Ding, M. Fieber-Erdmann, and T. Drewello, J. Chem. Phys. **104**, 2548 (1996).
[31] A. Kramida, Yu. Ralchenko, J. Reader, and NIST ASD Team, NIST atomic spectra database (ver. 5.2) (National Institute of Standards and Technology, Gaithersburg, 2014), http://physics.nist.gov/asd.
[32] C. C. Wang, O. Kornilov, O. Gessner, J. H. Kim, D. S. Peterka, and D. M. Neumark, J. Phys. Chem. **112**, 9356 (2008).
[33] F. Trinter *et al.*, Phys. Rev. Lett. **111**, 233004 (2013).
[34] A. A. Scheidemann, V. V. Kresin, and H. Hess, J. Chem. Phys. **107**, 2839 (1997).
[35] G. Marr and J. West, At. Data Nucl. Data Tables **18**, 497 (1976).
[36] Y. Ren and V. V. Kresin, Phys. Rev. A **76**, 043204 (2007).
[37] F. Reuse, S. N. Khanna, V. de Coulon, and J. Buttet, Phys. Rev. B **41**, 11743 (1990).
[38] T. Diederich, T. Döppner, T. Fennel, J. Tiggesbäumker, and K.-H. Meiwes-Broer, Phys. Rev. A **72**, 023203 (2005).
[39] J. Eland, Laser Chem. **11**, 259 (1991).
[40] See Supplemental Material http://link.aps.org/supplemental/10.1103/PhysRevLett.116.203001, which includes Refs. [41–47], for (i) additional experimental data complimentary to that shown in the manuscript and (ii) a brief theoretical discussion along with computed ETMD electron energies for different complex configurations.
[41] H. Werner, P. Knowles, G. Knizia, F. Manby, M. Schütz, P. Celani, T. Korona, R. Lindh, A. Mitrushenkov, G. Rauhut *et al.*, https://www.molpro.net/.
[42] D. E. Woon and T. H. Dunning Jr., J. Chem. Phys. **100**, 2975 (1994).
[43] K. L. Schuchardt, B. T. Didier, T. Elsethagen, L. Sun, V. Gurumoorthi, J. Chase, J. Li, and T. L. Windus, J. Chem. Inf. Model. **47**, 1045 (2007).
[44] A. Trofimov and J. Schirmer, J. Chem. Phys. **123**, 144115 (2005).
[45] J. Schirmer and A. Barth, Z. Phys. A **317**, 267 (1984).
[46] F. Tarantelli, Chem. Phys. **329**, 11 (2006).
[47] G. Karlström, R. Lindh, P.-Å. Malmqvist, B. O. Roos, U. Ryde, V. Veryazov, P.-O. Widmark, M. Cossi, B. Schimmelpfennig, P. Neograd *et al.*, Comput. Mater. Sci. **28**, 222 (2003).